Analysing powers of the $\vec{d}p \to \vec{d}p$ reaction at 1.2 and 2.27 GeV

David Mchedlishvili *for the ANKE collaboration*

November 23, 2013

Abstract

Vector and tensor analysing powers of the $\vec{d}p \to \vec{d}p$ reactions were measured at $T_d = 1.2$ and 2.27 GeV beam energies using the ANKE experimental data from November 2006 beam time. Results at 1.2 GeV are in good agreement with older ANKE measurement at 1.17 GeV and with SATURNE and Argonne data at energies very close to that. Therefore, data at 1.2 GeV provide consistency check of the polarimetry, as well as the analysis technique itself. Since no other measurement exists at 2.27 GeV, the ANKE data is compared with Argonne measurements at 2 GeV. The qualitative agreement is achieved.

The polarised differential cross section $d\sigma(\vartheta,\varphi)$ of the deuteron-proton elastic scattering is expressed in terms of polarisation observables in the following way:

$$\frac{d\sigma(\vartheta,\varphi)}{d\sigma_0(\vartheta)} = 1 + \tfrac{3}{2}P_z A_y(\vartheta)\cos\varphi + \tfrac{1}{4}P_{zz}[A_{x,x}(\vartheta)(1-\cos 2\varphi) + A_{y,y}(\vartheta)(1+\cos 2\varphi)]\,, \qquad (1)$$

where $d\sigma_0(\vartheta)$ is unpolarised cross section, P_z and P_{zz} are beam vector and tensor polarisations, respectively. The vector (A_y) and tensor (A_{xx}, A_{yy}) analysing powers are to be measured.

Eight configurations of the polarise deuteron ion source at COSY were used in the 2006 experiment, with different vector and tensor polarisations. Their ideal and measured values are listed in table 1. Beam P_z vector polarisations were measured using the quasi-free $np \to d\pi^0$ reaction, while P_{zz} tensor polarisations were obtained from the deuteron-proton charge-exchange reaction at 1.2 GeV flat top. Note, that due to the large difference in the cross sections of these processes the tensor polarisations have been determined with much better accuracy.

Mode	P_z	P_{zz}	P_z by LEP	P_z by ANKE	P_{zz} by ANKE
1	$-\frac{2}{3}$	0	-0.541 ± 0.008	-0.522 ± 0.053	0.004 ± 0.021
2	$+\frac{1}{3}$	-1	0.197 ± 0.008	0.307 ± 0.056	-0.548 ± 0.022
3	$-\frac{1}{3}$	$+1$	-0.331 ± 0.011	-0.382 ± 0.053	0.498 ± 0.022
4	0	$+1$	0.031 ± 0.009	-0.024 ± 0.056	0.558 ± 0.019
5	-1	$+1$	-0.758 ± 0.007	-0.746 ± 0.052	0.524 ± 0.019
6	$+1$	$+1$	0.659 ± 0.008	0.676 ± 0.058	0.411 ± 0.020
7	0	-2	-0.491 ± 0.012	-0.255 ± 0.057	-0.228 ± 0.022
8	0	0	-0.007 ± 0.010	–	–

Table 1: The table lists beam vector and tensor polarisation measurement results for eight different configurations of the polarised deuteron ion source together with LEP and ANKE measurements during November 2006 beam time.

The $\vec{d}p \to \vec{d}p$ process (with fast deuteron in the forward) was identified from the single particle momentum spectrum. Since in the forward direction the scattered deuteron has momenta very close to the beam initial momentum, the corresponding missing mass spectra (shown in Fig. 1) are very clean, with no background.

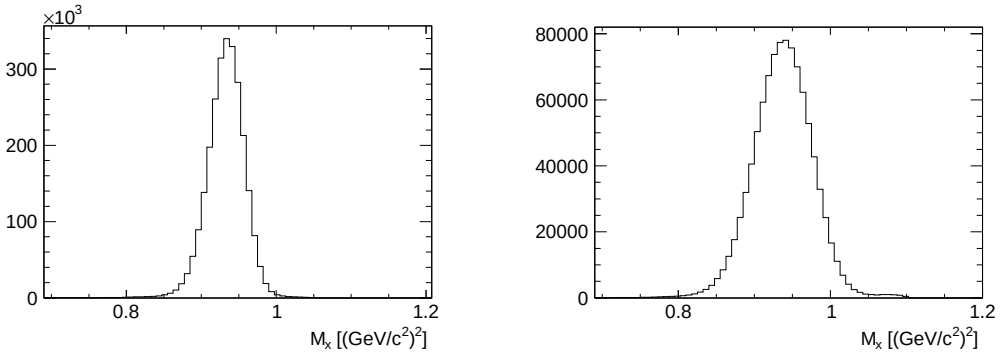

Figure 1: The missing mass spectra for the identified deuteron at 1.2 (left) and 2.27 GeV (right).

It should be noted that the polarised cross section of Eq. 1 is significantly more sensitive to vector polarisation effects rather than tensor. This leads to some complications in determining the tensor analysing powers in presence of vector polarisation. Since almost every polarisation state of Table 1 was vector polarised, it became necessary to combine at least two different modes to cancel out the vector polarisation effect. Unfortunately, the precision of ANKE P_z measurements

involving the quasi-free $np \to d\pi^0$ reaction is not enough to well determine the weights of the two states. Because of that the P_z values measured at ANKE were calibrated by LEP results. The comparison of these two measurements are shown in Fig. 2.

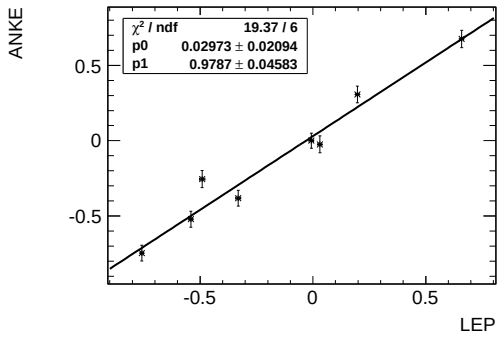

Figure 2: The comparison of P_z results measured at ANKE and at LEP.

The calibrated values of P_z are listed in Table 2 (left). These values were then used to correctly determine the weights for different states with opposite vector polarisations. Tensor polarisations of the combined states were then remeasured (right table).

Mode	Calibrated P_z
1	-0.500 ± 0.033
2	0.223 ± 0.024
3	-0.294 ± 0.028
4	0.060 ± 0.023
5	-0.712 ± 0.041
6	0.675 ± 0.038
7	-0.451 ± 0.033
8	0.023 ± 0.023

Mode set	P_{zz}
5, 6	0.465 ± 0.017
2, 7	-0.443 ± 0.020
4, 3	0.548 ± 0.017

Table 2: The left table lists calibrated vector polarisations for eight different configurations of the polarised deuteron ion source. States with opposite vector polarisations are summed with weights defined from the calibrated P_z values to cancel the vector polarisation effects. Resulted tensor polarisations of such sets of polarised states are listed in the right table.

The A_y vector analysing power was obtained by fitting the normalised $cos2\varphi$ distribution using only polarised state 1, where the tensor polarisation was found to be zero. Results are presented in Fig. 3 as functions of deuteron CM scattering angle together with other data, obtained at close energies. The vector analysing power signal at 2.27 GeV is significantly smaller than at 1.2 GeV (numerical values are listed in Table 3), and is also smaller than that measured at Argonne at 2 GeV. This is in agreement with Argonne data at 1.2, 1.6 and 2 GeV, that clearly show a dilution of the vector analysing power signal as energy increases.

The A_{xx} and A_{yy} tensor analysing powers were determined separately for different sets of combined polarised states, listed in Table 2, and then results were averaged over these sets. The final results are shown in Fig. 4 and Fig. 5 as functions of deuteron CM scattering angle. Similarly to A_y, the new results for A_{yy} well agrees with existing data at 1.2 GeV. At 2.27 GeV, the difference from Argonne data at 2 GeV is negligible, at least up to 27 degrees in CM, if the error bars are taken into account. Nevertheless, it should be noted, that the zero-crossing point tends to move towards the smaller angles as energy increases. This effect can be easily observed in Argonne data at 1.2, 1.6 and 2 GeV, and is also demonstrated by new ANKE results. Due to a very asymmetric acceptance of the ANKE forward detector the φ coverage of the fast deuteron is such that mainly the A_{yy} can be measured. Nevertheless, information on A_{xx} was also obtained, though with much

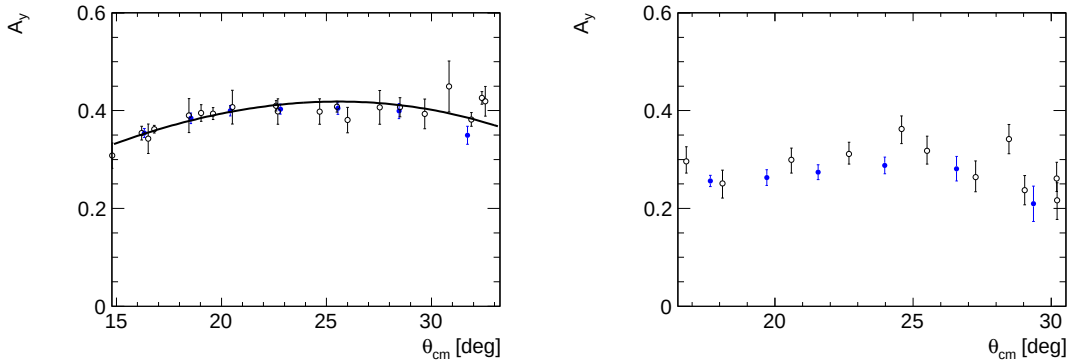

Figure 3: New ANKE results (closed points) for the vector analysing powers of the $\vec{d}p \to \vec{d}p$ reaction at 1.2 (left) and 2.27 GeV (right). The error bars do not include 7% beam polarisation uncertainty. New results are compared with existing measurements at close energies (open points) including SATURNE at 1198 MeV, Argonne at 1194 and 2000 MeV, and ANKE at 1170 MeV (numerical values are listed in Tables 4, 5, 6, 7). In the left figure the overall fit with polynomial is also shown (not including new results).

worse accuracy.

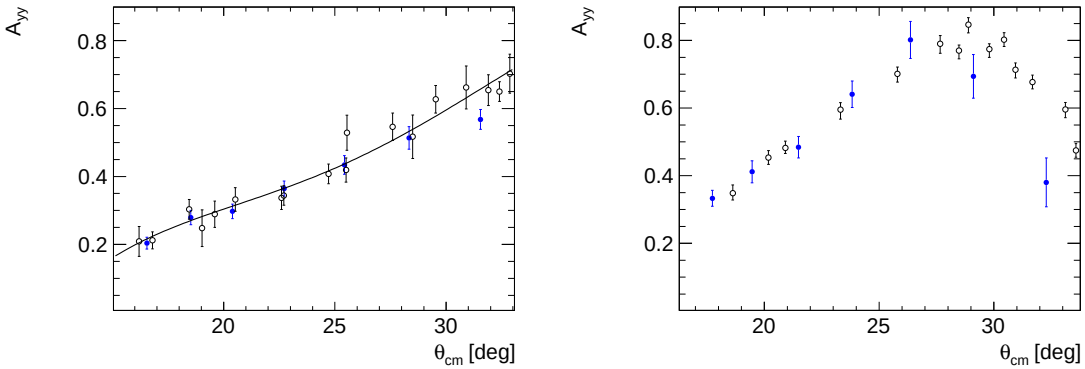

Figure 4: New ANKE results (closed points) for the A_{yy} tensor analysing powers of the $\vec{d}p \to \vec{d}p$ reaction at 1.2 (left) and 2.27 GeV (right). The error bars include uncertainties arising from the beam polarimetry. New results are compared with existing measurements at close energies (open points) including SATURNE at 1198 MeV, Argonne at 1194 and 2000 MeV, and ANKE at 1170 MeV. In the left figure the overall fit with polynomial is also shown (not including new results).

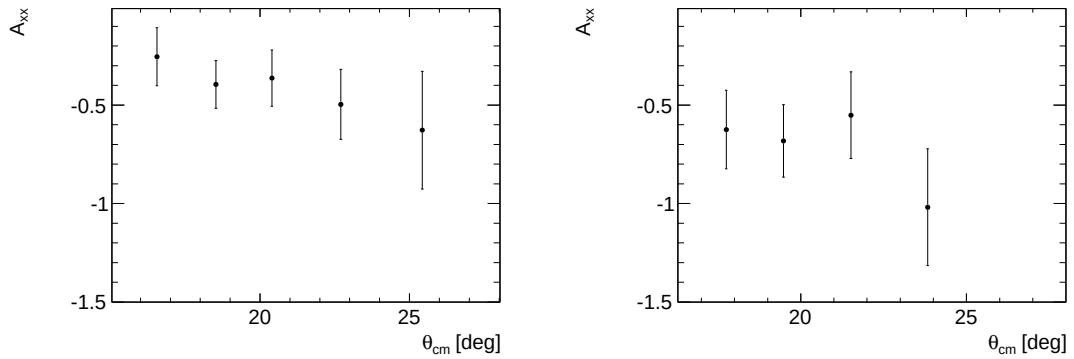

Figure 5: New ANKE results for the A_{xx} tensor analysing powers of the $\vec{d}p \to \vec{d}p$ reaction at 1.2 (left) and 2.27 GeV (right). The error bars include uncertainties arising from the beam polarimetry.

T_d	ϑ_{cm}	A_y	A_{yy}
1.2 GeV	16.3	0.354 ± 0.009	0.204 ± 0.017
	18.5	0.384 ± 0.011	0.279 ± 0.021
	20.4	0.400 ± 0.011	0.297 ± 0.021
	22.8	0.403 ± 0.010	0.365 ± 0.022
	25.5	0.405 ± 0.013	0.434 ± 0.027
	28.5	0.399 ± 0.015	0.514 ± 0.033
	31.7	0.350 ± 0.019	0.567 ± 0.029
2.27 GeV	17.7	0.256 ± 0.012	0.333 ± 0.023
	19.7	0.263 ± 0.016	0.411 ± 0.033
	21.6	0.274 ± 0.015	0.482 ± 0.032
	24.0	0.288 ± 0.017	0.640 ± 0.039
	26.6	0.281 ± 0.025	0.801 ± 0.055
	29.4	0.210 ± 0.036	0.692 ± 0.064
	32.5	0.045 ± 0.045	0.380 ± 0.072

Table 3: The table lists vector and tensor analysing powers of the $\vec{d}p \to \vec{d}p$ reaction measured at ANKE.

ϑ_{cm}	A_y	A_{yy}
16.2	0.354 ± 0.014	0.209 ± 0.044
16.8	0.362 ± 0.008	0.212 ± 0.025
19.0	0.395 ± 0.017	0.248 ± 0.054
19.6	0.394 ± 0.012	0.289 ± 0.039
22.6	0.410 ± 0.011	0.337 ± 0.034
25.5	0.408 ± 0.011	0.419 ± 0.035
28.5	0.407 ± 0.020	0.517 ± 0.064
31.9	0.382 ± 0.014	0.654 ± 0.045

Table 4: The table lists vector and tensor analysing powers of the $\vec{d}p \to \vec{d}p$ reaction measured at ANKE at 1.17 GeV.

ϑ_{cm}	A_y	A_{yy}
32.4	0.426 ± 0.013	0.650 ± 0.029
35.8	0.333 ± 0.028	0.795 ± 0.038
37.9	0.253 ± 0.008	0.876 ± 0.008
39.3	0.289 ± 0.022	0.825 ± 0.036
42.1	0.167 ± 0.030	–
71.2	0.115 ± 0.023	-0.465 ± 0.025
77.0	0.142 ± 0.023	-0.369 ± 0.026
83.0	0.161 ± 0.040	-0.366 ± 0.042
93.9	0.073 ± 0.026	-0.158 ± 0.028

Table 5: The table lists vector and tensor analysing powers of the $\vec{d}p \to \vec{d}p$ reaction measured at SATURNE at 1198 MeV.

ϑ_{cm}	A_y
10.6	0.261 ± 0.017
12.9	0.286 ± 0.017
14.8	0.308 ± 0.026
16.5	0.342 ± 0.030
18.5	0.390 ± 0.035
20.5	0.407 ± 0.035
22.7	0.398 ± 0.026
24.7	0.398 ± 0.026
26.0	0.381 ± 0.026
27.5	0.407 ± 0.035
29.7	0.393 ± 0.030
30.8	0.449 ± 0.052
32.6	0.419 ± 0.030
34.4	0.367 ± 0.026
35.4	0.289 ± 0.039
36.9	0.323 ± 0.035
37.7	0.302 ± 0.030
39.3	0.323 ± 0.043
42.9	0.193 ± 0.035
46.3	0.084 ± 0.030
48.2	0.002 ± 0.035
51.1	-0.059 ± 0.030
51.3	-0.098 ± 0.030
56.1	0.018 ± 0.030
61.2	0.052 ± 0.035

ϑ_{cm}	A_{yy}
18.5	0.303 ± 0.029
20.5	0.332 ± 0.035
22.7	0.344 ± 0.029
24.7	0.408 ± 0.029
25.5	0.529 ± 0.052
27.6	0.546 ± 0.040
29.5	0.627 ± 0.040
30.9	0.662 ± 0.063
32.9	0.703 ± 0.058
34.5	0.824 ± 0.046
35.5	0.726 ± 0.058
37.1	0.842 ± 0.063
37.7	0.928 ± 0.052
39.3	0.900 ± 0.063
43.1	0.825 ± 0.052
46.4	0.618 ± 0.046
48.1	0.527 ± 0.040
51.1	0.262 ± 0.052
51.2	0.118 ± 0.029
56.3	-0.325 ± 0.040
61.4	-0.479 ± 0.040

Table 6: The left and right tables list vector and tensor analysing powers of the $\vec{d}p \to \vec{d}p$ reaction, respectively. Measurements have been performed at Argonne at 1194 MeV.

ϑ_{cm}	A_y
12.2	0.203 ± 0.028
13.9	0.251 ± 0.032
16.8	0.296 ± 0.027
18.1	0.251 ± 0.028
20.6	0.299 ± 0.025
22.7	0.311 ± 0.022
24.6	0.362 ± 0.028
25.5	0.318 ± 0.028
27.3	0.264 ± 0.031
28.5	0.342 ± 0.030
29.0	0.237 ± 0.030
30.2	0.261 ± 0.030
30.2	0.217 ± 0.037
31.7	0.184 ± 0.025
33.3	0.163 ± 0.030
33.3	0.091 ± 0.025
35.2	0.106 ± 0.031
35.8	0.092 ± 0.027
38.5	0.059 ± 0.027
39.0	0.026 ± 0.025
40.4	0.104 ± 0.024
41.0	0.098 ± 0.027
43.4	0.162 ± 0.024
45.8	0.180 ± 0.024
48.5	0.267 ± 0.025
51.3	0.253 ± 0.028
54.1	0.316 ± 0.027
56.7	0.346 ± 0.027
58.8	0.326 ± 0.024
62.1	0.228 ± 0.027
64.2	0.348 ± 0.025
67.1	0.265 ± 0.024
69.4	0.337 ± 0.027
72.7	0.293 ± 0.025
73.3	0.341 ± 0.022

ϑ_{cm}	A_{yy}
13.2	0.194 ± 0.022
14.8	0.271 ± 0.020
16.0	0.320 ± 0.020
18.6	0.348 ± 0.022
20.2	0.454 ± 0.020
20.9	0.482 ± 0.018
23.3	0.596 ± 0.025
25.8	0.701 ± 0.022
27.7	0.790 ± 0.026
28.5	0.770 ± 0.021
28.9	0.847 ± 0.022
29.8	0.774 ± 0.021
30.4	0.802 ± 0.020
30.9	0.713 ± 0.022
31.7	0.677 ± 0.020
33.1	0.596 ± 0.022
33.6	0.475 ± 0.020
33.8	0.442 ± 0.022
35.5	0.195 ± 0.022
35.7	0.163 ± 0.024
36.1	0.086 ± 0.026
38.9	-0.319 ± 0.024
39.2	-0.363 ± 0.026
40.6	-0.505 ± 0.043
41.1	-0.549 ± 0.030
43.5	-0.602 ± 0.036
45.9	-0.589 ± 0.034
48.5	-0.524 ± 0.032
51.5	-0.431 ± 0.030
54.1	-0.394 ± 0.032
56.9	-0.333 ± 0.034
58.9	-0.232 ± 0.033
62.3	-0.163 ± 0.030
64.5	-0.179 ± 0.030
67.4	-0.122 ± 0.032
69.5	-0.109 ± 0.034
73.0	-0.125 ± 0.030
73.6	-0.125 ± 0.030

Table 7: The left and right tables list vector and tensor analysing powers of the $\vec{d}p \to \vec{d}p$ reaction, respectively. Measurements have been performed at Argonne at 2000 MeV.